Buonocore, V., Poerio, E., Gramenzi, F., & Silano, V. (1975) *J. Chromatogr. 114*, 109-114.
Burrill, P. H., Brannon, P. M., & Kretchmer, N. (1981) *Anal. Biochem. 117*, 402-405.
Goto, A., Matsui, Y., Ohyama, K., Arai, M., & Murao, S. (1983) *Agric. Biol. Chem. 47*, 83-88.
Goto, A., Matsui, Y., Ohyama, K., Arai, M., & Murao, S. (1985a) *Agric. Biol. Chem. 49*, 435-439.
Goto, A., Arai, M., & Murao, S. (1985b) *Nippon Nogei Kagaku Kaishi 59*, 411-417.
Hartley, B. S. (1970) *Biochem. J. 119*, 805-822.
Hirayama, K., Ando, T., Takahashi, R., & Murai, A. (1986) *Bull. Chem. Soc. Jpn. 59*, 1371-1378.
Hofmann, O., Vértesy, L., & Braunitzer, G. (1985) *Biol. Chem. Hoppe-Seyler 366*, 1161-1168.
Kline, A. D., & Wüthrich, K. (1985) *J. Mol. Biol. 183*, 503-507.
Kline, A. D., Braun, W., & Wüthrich, K. (1986) *J. Mol. Biol. 189*, 377-382.
Kluh, I. (1981) *FEBS Lett. 136*, 231-234.
Maeda, K., Hase, T., & Matsubara, H. (1983) *Biochim. Biophys. Acta 743*, 52-57.
Marshall, J. J., & Lauda, C. M. (1975) *J. Biol. Chem. 250*, 8030-8037.
Murai, H., Hara, S., Ikanaka, T., Goto, A., Arai, M., & Murao, S. (1985) *J. Biochem. (Tokyo) 97*, 1129-1133.
Murao, S., Goto, A., Matsui, Y., & Ohyama, K. (1980a) *Agric. Biol. Chem. 44*, 1679-1681.
Murao, S., Goto, A., & Arai, M. (1980b) *Agric. Biol. Chem. 44*, 1683-1684.
Murao, S., Goto, A., Matsui, Y., Ohyama, K., & Arai, M. (1981) *Agric. Biol. Chem. 45*, 2599-2604.
Murao, S., Oouchi, N., Goto, A., & Arai, M. (1983) *Agric. Biol. Chem. 47*, 453-454.
Murao, S., Oouchi, N., Goto, A., & Arai, M. (1985) *Agric. Biol. Chem. 49*, 107-110.
Nakajima, R., Imanaka, T., & Aiba, S. (1986) *Appl. Microbiol. Biotechnol. 23*, 355-360.
O'Donnell, M. D., FitzGerald, O., & McGeeney, K. F. (1977) *Clin. Chem. (Winston-Salem, N.C.) 23*, 560-566.
Oouchi, N., Arai, M., & Murao, S. (1985) *Agric. Biol. Chem. 49*, 793-797.
Pflugrath, J. W., Wiegand, G., & Huber, R. (1986) *J. Mol. Biol. 189*, 383-386.
Samy, T. S. A., Hahm, K.-S., Modest, E. J., Lampman, G. W., Keutmann, H. T., Umazawa, H., Herlihy, W. C., Gibson, B. W., Carr, S. A., & Biemann, K. (1983) *J. Biol. Chem. 258*, 183-191.
Thoma, J. A., Spradlin, J. E., & Dygert, S. (1971) *Enzymes (3rd Ed.) 5*, 115.
Vértesy, L., & Tripier, D. (1985) *FEBS Lett. 185*, 187-190.
Vértesy, L., Oeding, V., Bender, R., Zepf, K., & Nesemann, G. (1984) *Eur. J. Biochem. 141*, 505-512.
Weiner, A. M., Platt, T., & Weber, K. (1972) *J. Biol. Chem. 247*, 3242-3251.
Yazdanparast, R., Anderews, P., Smith, D. L., & Dixon, J. E. (1986) *Anal. Biochem. 153*, 348-353.
Yergey, J., Heller, D., Hansen, G., Cotter, R. J., & Fenselau, C. (1983) *Anal. Chem. 55*, 353-356.

Amide Proton Exchange in the α-Amylase Polypeptide Inhibitor Tendamistat Studied by Two-Dimensional ^{1}H Nuclear Magnetic Resonance†

Wang Qiwen,‡ Allen D. Kline, and Kurt Wüthrich*
Institut für Molekularbiologie und Biophysik, Eidgenössische Technische Hochschule Zürich-Hönggerberg, CH-8093 Zürich, Switzerland
Received March 27, 1987

ABSTRACT: The individual amide proton exchange rates in Tendamistat at pH 3.0 and 50 °C were measured by using two-dimensional ^{1}H nuclear magnetic resonance. Overall, it was found that the distribution of exchange rates along the sequence is dominated by the interstrand hydrogen bonds of the β-sheet structures. The slowly exchanging protons in the core of the two β-sheets were shown to exchange via an EX2 mechanism. Further analysis of the data indicates that different large-scale structure fluctuations are responsible for the exchange from the two β-sheets, even though the three-dimensional structure of Tendamistat appears to consist of a single structural domain.

Tendamistat (HOE-467) is an effective polypeptide inhibitor of mammalian α-amylases (Aschauer et al., 1981; Vértesy et al., 1984). Its binding activity appears to be related to the presence of a specific sequence of Trp-Arg-Tyr (Murai et al., 1985; Vértesy & Tripier, 1985). The conformation of this peptide segment as well as the overall backbone fold of Tendamistat was determined independently by X-ray diffraction in single crystals (Pflugrath et al., 1986) and by nuclear magnetic resonance (NMR)[1] in solution (Kline & Wüthrich, 1985; Kline et al., 1986). These features of the protein coincide closely in the crystal and in solution, with the polypeptide backbone forming an antiparallel β-barrel of six strands. In this paper, the investigations on Tendamistat are extended to

† This work was supported by the Schweizerischer Nationalfonds (Project 3.198-0.85).
‡ Permanent address: Shanghai Institute of Organic Chemistry, Academia Sinica, Shanghai, China.

[1] Abbreviations: NMR, nuclear magnetic resonance; 2D, two dimensional; COSY, 2D correlated spectroscopy; 2QF-COSY, two-quantum-filtered COSY; NOESY, 2D nuclear Overhauser enhancement spectroscopy.

0006-2960/87/0426-6488$01.50/0

dynamic properties of the solution conformation. The 70 amide protons in Tendamistat were examined for their exchange rates with deuterium of the solvent ^2H_2O, using 2D NMR techniques capable of providing the resolution needed to measure the exhange rates at individual sites in the protein (Wagner & Wüthrich, 1982; Wüthrich, 1986). This information was combined with the sequence-specific ^1H NMR assignments (Kline & Wüthrich, 1986) to obtain information on the spatial distribution of internal motions in the three-dimensional protein structure. The data are discussed in terms of transient structure fluctuations responsible for the observed exchange.

Materials and Methods

Two different sets of amide proton exchange measurements were carried out. In the first experiments, a sample of the dry protein was first mixed with ^2H_2O. The resulting p^{2}H value corresponds to the isoelectric point for Tendamistat, and the protein remained undissolved. The ^2H_2O was removed once by lyophilization. Then a 3 mM solution of the protein in 99.8% ^2H_2O was prepared by titrating the p^{2}H to 3.0 with a deuteriated perchloric acid solution. No extra salt, buffer, or base was added to this protein solution, and it was stored at 4 °C. Eight NMR samples were removed from the stock solution and heated to 50 (±0.5) °C for 0, 5, 20, 100, 240, 480, 1020, and 4200 min, respectively. After the exchange at 50 °C during the indicated time, 2QF-COSY spectra were recorded on a Bruker WM-500 spectrometer with the probe temperature at 25 °C, with an overall recording time of 11 h per spectrum. Prior to Fourier transformation, the 400 t_1 values were zero-filled to 1024 points, while the 700 data points in t_2 were filled to 2048 points.

In the second exchange experiments, 16.0 mg of dry Tendamistat was dissolved in 0.5 mL of 99.8% ^2H_2O at 4 °C by adding 12.8 μL of a deuteriated perchloric acid solution (the amount of acid was preset by titrating a similar sample to pH 3.0; pH meter readings taken on all these samples after completion of the NMR experiment gave values of 3.0 ± 0.05 pH units). Immediately after the samples were heated to 50 (±0.5) °C for 0, 5, 20, or 80 min, NOESY spectra were collected on a Bruker WM-500 spectrometer with the probe temperature at 20 °C and an overall recording time of 11 h per spectrum. The 420 t_1 values were zero-filled to 1024 points, while the 1024 t_2 points were filled to 2048 points.

Previously, complete sequence-specific assignments were obtained for the ^1H NMR spectrum of Tendamistat at 50 °C (Kline & Wüthrich, 1986). Starting from these data, assingments were now also obtained for 20 and 25 °C, at which temperatures the spectra for the present exchange studies were recorded. For this, several samples were prepared in H_2O, and 2QF-COSY and NOESY spectra were recorded at 15, 37, and 50 °C, whereby the solvent signal was suppressed by selective preirradiation (Wider et al., 1983). All spectra in ^2H_2O and H_2O were collected and computed in the phase-sensitive mode.

For the determination of the experimental exchange rate constants, the ω_2 cross sections of the NH–αH COSY cross-peaks or selected NOESY cross-peaks with NH were individually plotted and evaluated for the peak intensity. Scrutinizing nonexchanging cross-peaks allowed an internal, relative calibration of the peak intensities in the different spectra. The height measurements were used as input for a nonlinear least-squares routine, which fitted both the zero point and the apparent first-order rate constant of the amide proton exchange.

Intrinsic exchange rate constants for the Tendamistat amino acid sequence were calculated by using the procedure of Molday et al. (1972) [see also Roder et al. (1985b)]. In this calculation, tryptophan was treated the same as phenylalanine, and the Asp and Glu residues were calculated as having pK_a's of 3.9 and 4.3, respectively.

Results

A key step in performing a 2D NMR amide proton exchange study (Wagner & Wüthrich, 1982) is finding suitable "quench" conditions. This amounts to a compromise between having interpretable NMR spectra and minimum exchange during the NMR measurement. For slow exchange rates, pH values near 3.5 (Wüthrich, 1986) and low temperature are best. For Tendamistat, a temperature of 50 °C and pH 3.2 were chosen for the initial ^1H NMR assignments (Kline & Wüthrich, 1986) and the structural studies (Kline & Wüthrich, 1985; Kline et al., 1986). 2QF-COSY spectra of a freshly prepared 7 mM ^2H_2O solution of the protein at p^{2}H 3.2 and 50 °C showed 27 NH–αH cross-peaks (Kline & Wüthrich, 1985). However, when a similar spectrum of the same solution was collected with a probe temperature of 25 °C, only about eight NH–αH cross-peaks could be found. The simultaneous absence cross-peaks corresponding to nonlabile protons in the aliphatic region indicated that the cause of the poor intensity was the increased line width of the NMR signals (Neuhaus et al., 1985). We therefore lowered the protein concentration to 3 mM. Under these conditions, adequate resolution was obtained, and numerous individual cross-peaks with amide protons could be identified in both 2QF-COSY and NOESY (see Figure 1). The complete spectral assignments of all amide protons in Tendamistat at 20 °C (Table I) were the result of a systematic study of NOESY spectra from 50 to 15 °C, which is being used for the structural work on Tendamistat. The chemical shifts were assigned by following the cross-peaks through the different temperatures. Throughout the temperature range, the same sets of peaks were observed, which precludes any major conformational changes. On this basis, the assignments were also confirmed independently by relating 2QF-COSY spectra in H_2O and in ^2H_2O to the complete assignments at 50 °C.

The measurements of proton-to-deuterium exchange rates were performed on the exchange series with both NOESY and 2QF-COSY, as described under Materials and Methods. For the majority of the amide protons, the exchange could be followed by examining the 2QF-COSY spectra. In other cases, however, excessive overlap or vanishing intensities due to small couplings, $^3J_{HN\alpha}$ (Neuhaus et al., 1985), made the COSY peak intensities unmeasurable. Here the NOESY spectra proved useful. NOESY spectra of proteins typically contain more cross-peaks for a given amide than do COSY-type spectra. Thus, the larger selection usually ensures that one or several resolved NOESY cross-peaks can be found for any amide proton. Instead of the cancellation effects in COSY spectra due to small coupling constants, NOESY cross-peaks with small fine structure splittings are even easier to detect above the noise. The complementary nature of NOESY and COSY was thus used to identify cross-peaks with all amide protons that had not completely exchanged within the dead time of our experiment. Though all amide protons in Tendamistat were identified in H_2O spectra, 16 of them were never seen in ^2H_2O because they exchange too fast to be detected by our experimental setup. As a consequence, only a lower limit for the exchange rates of these protons was obtained (Table I).

By keeping the experimental conditions identical for all spectra in an exchange series, the change of the cross-peak intensities is only a function of the proton-to-deuterium exchange rate (Wagner & Wüthrich, 1982). By following the

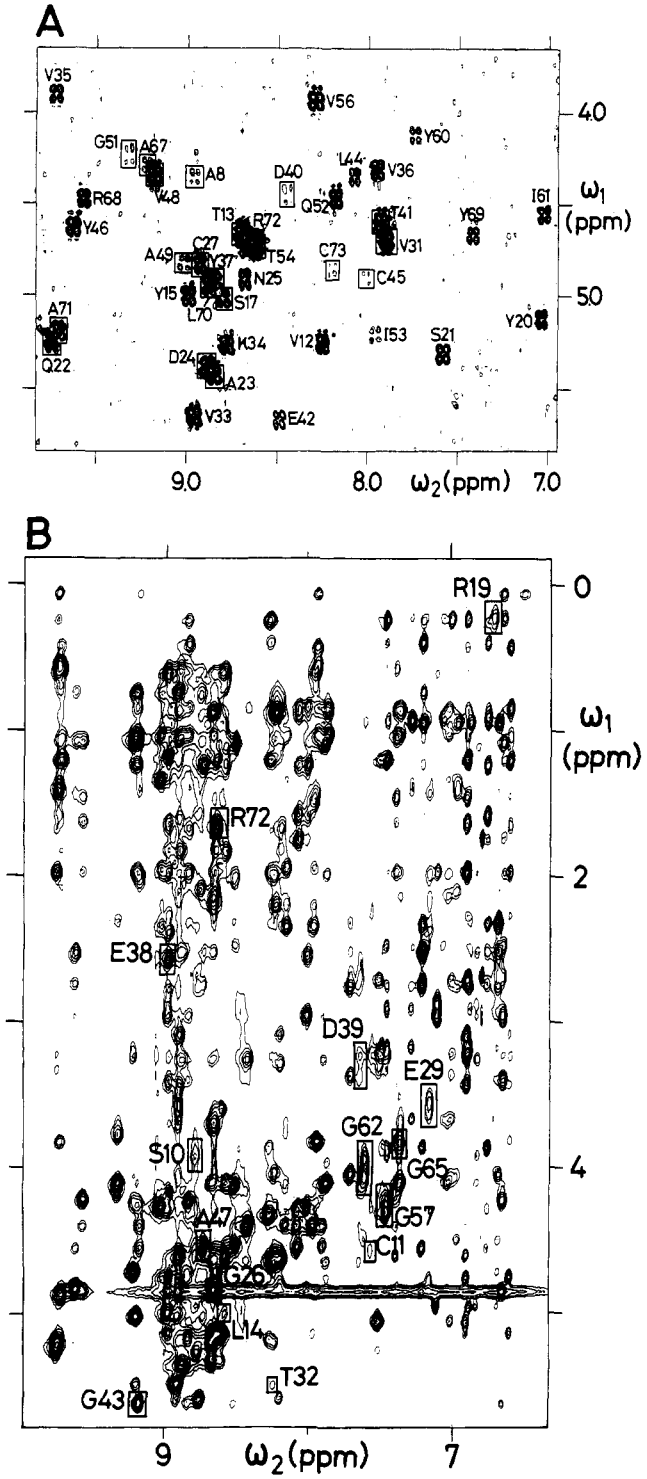

FIGURE 1: Regions in 2D ^1H NMR spectra of freshly prepared ^2H_2O solutions of Tendamistat. (A) The fingerprint region (ω_1 = 3.5–5.8 ppm, ω_2 = 6.9–9.8 ppm) of a 2QF-COSY spectrum contains 40 NH–αH cross-peaks, which are labeled with the amino acid type and the sequence position. Positive and negative intensities were plotted without distinction in this phase-sensitive spectrum. The peaks in crowded regions have been boxed to illustrate the spectral interpretation. (B) The region (ω_1 = −0.2 to 5.8 ppm, ω_2 = 6.3–10.0 ppm) of a NOESY spectrum at 20 °C provided evidence for the presence of 14 additional amide protons not seen in (A) (note that the resonance of Arg-72 is identified in both spectra). Representive cross-peaks for these amide protons are boxed and labeled. In this spectrum, a polynomial base-line correction was performed in both dimensions.

intensity change with exchange time, it was possible to determine the apparent first-order rate constants. Spectral quantitation was performed by plotting identical cross sections through the spectra recorded after different exchange times.

Table I: Chemical Shifts (p^2H 3.0, 20 °C, ppm ± 0.02) and Exchange Rate Constants (min^{-1} at 50 °C and p^2H 3.0) of the Amide Protons in Tendamistat

residue	δ_{NH} (ppm)	k_m[a] (×10^{-3} min^{-1})	residue	δ_{NH} (ppm)	k_m[a] (×10^{-3} min^{-1})
Thr-2	8.74[b]	>400	Asp-39	7.64	200*
Thr-3	8.36[b]	>400	Asp-40	8.41	100*
Val-4	8.25[b]	>400	Thr-41	7.89	6.3
Ser-5	8.44[b]	>400	Glu-42	8.49	30*
Glu-6	8.65[b]	>400	Gly-43	9.15	30*
Ala-8	8.96	7*	Leu-44	8.07	10*
Ser-10	8.76	400*	Cys-45	8.00	30*
Cys-11	7.56	200*	Tyr-46	9.59	0.20
Val-12	8.21	0.76	Ala-47	8.71	30*
Thr-13	8.65	0.26	Val-48	9.18	0.078
Leu-14	8.56	20*	Ala-49	9.00	8*
Tyr-15	8.95	0.23	Gly-51	9.30	6*
Gln-16	8.90[b]	>400	Gln-52	8.14	1.7
Ser-17	8.75	5.0	Ile-53	7.95	20*
Trp-18	8.35[b]	>400	Thr-54	8.60	0.59
Arg-19	6.72	400*	Thr-55	8.76[b]	>400
Tyr-20	6.99	10*	Val-56	8.24	0.19
Ser-21	7.51	1.2	Gly-57	7.44	3*
Gln-22	9.73	0.59	Asp-58	8.85[b]	>400
Ala-23	8.81	0.38	Gly-59	8.47[b]	>400
Asp-24	8.86	1.1	Tyr-60	7.70	8*
Asn-25	8.65	2.6	Ile-61	6.96	7*
Gly-26	8.64	5*	Gly-62	7.61	200*
Cys-27	8.88	0.81	Ser-63	8.36[b]	>400
Ala-28	8.39[b]	>400	His-64	8.37[b]	>400
Glu-29	7.15	100*	Gly-65	7.36	100*
Thr-30	8.64[b]	>400	His-66	8.95[b]	>400
Val-31	7.87	0.18	Ala-67	9.19	20*
Thr-32	8.22	100*	Arg-68	9.54	8*
Val-33	8.89	0.081	Tyr-69	7.38	0.50
Lys-34	8.72	0.24	Leu-70	8.88	2.4
Val-35	9.71	0.10	Ala-71	9.68	0.20
Val-36	7.93	0.040	Arg-72	8.63	1*
Tyr-37	8.81	0.16	Cys-73	8.18	30*
Glu-38	8.95	4*	Leu-74	8.20[b]	>400

[a] The standard deviation of k_m was less than 10%, except for the values identified with an asterisk, where only approximate exchange rates were obtained for reasons described in the text, and for the residues where only a lower limit for k_m is indicated. [b] No peak was seen in D_2O at 20 °C. The chemical shift at 20 °C was extrapolated from two measurements in H_2O at 15 and 37 °C.

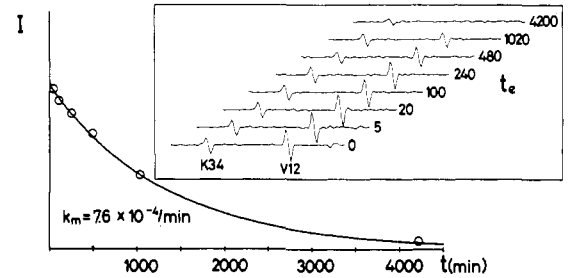

FIGURE 2: Cross sections parallel to the ω_2 axis at ω_1 = 5.23 ppm taken from 2QF-COSY spectra (Figure 1) recorded at different times after Tendamistat was dissolved in ^2H_2O. The cross sections show the peak intensities for Val-12 and Lys-34. The scaling and plot parameters are identical in all eight cross sections. In the lower part of the figure, the peak intensity for Val-12 is plotted vs. the exchange time. The curve was determined by a nonlinear least-squares fit of the experimental data and corresponds to the k_m value given in the figure.

Figure 2 shows a series of cross sections taken from 2QF-COSY, where the individual changes of the resonance intensities (measured as the peak-to-peak heights of the antiphase signals) for Val-12 and Lys-34 can be followed. The exchange rate was calculated to be 7.6 × 10^{-4} min^{-1} at 50 °C by using the Val-12 data. A fit of the experimental data is also shown in Figure 2. In a similar manner, the cross sections for a total

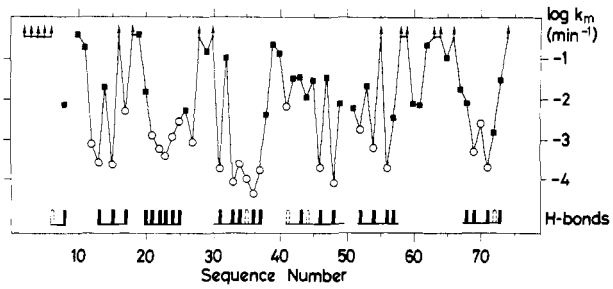

FIGURE 3: Plot of the logarithm of the amide proton exchange rates vs. the amino acid sequence of Tendamistat. Circles indicate rates calculated from five or more data points and represent the most accurately determined rate values (see text and Table I). Squares indicate rates obtained from fewer than five data points and represent an estimate for k_m. The arrows toward the top of the plot indicate those amide protons which were observed in H_2O but never detected in ^2H_2O solutions, so that only a lower limit for k_m can be given. For easy recognition of patterns of exchange rates along the sequence, the k_m values of sequentially neighboring amide protons were connected by straight lines. At the bottom, the locations of the β-sheet secondary structures and the amide protons involved in interstrand hydrogen bonds are identified by solid or dashed bars. The dashed lines are those hydrogen bonds implicated by the secondary structure analysis (Kline & Wüthrich, 1985), for which the hydrogen receptor group could not be unambiguously identified with the available NOE distance constraints.

of 54 amide protons are listed in Table I. Where at least five nonzero intensity values could be quantitated, the standard deviation for the exchange rate constant, k_m, was always less than 10%. For those amide protons showing up exclusively in the first few spectra, only estimates for the rate constants were obtained, as indicated in the table.

In a different presentation of the data in Table I, Figure 3 shows a plot of the exchange rates vs. the sequence number. From this plot, the individual β-strands of Tendamistat (Kline & Wüthrich, 1985; Kline et al., 1986; Pflugrath et al., 1986) can be classified according to their amide proton exchange patterns. The strand 20–25 contains only slowly exchanging amide protons. The same holds for the strand 30–37, except for residues 30–32. The strands 12–17, 41–49, and 52–58 have picket fence patterns with alternation of slow and fast exchange. [These regular patterns are locally disturbed by the presence of nonregular features in the β-sheets, such as β-bulges or near turns (Kline & Wüthrich, 1985).] The strand 67–73 has slowed exchange with a less well-defined pattern, which is nonetheless reminiscent of a picket fence. At the bottom of the plot are indicated the hydrogen bonds identified during the determination of the chainfold (Kline & Wüthrich, 1985).

Discussion

Examination of the plot of the exchange rates vs. the amino acid sequence (Figure 3) shows that the hydrogen bonding within the β-sheets is the primary factor determining the amide proton exchange for Tendamistat. The individual strands in the β-structures demonstrate two different patterns, i.e., either alternation of fast and slow exchange along the amino acid sequence or slow exchange throughout. Similar patterns were previously found to be consistent with the hydrogen bonding identified in antiparallel β-sheets of different proteins (Wagner & Wüthrich, 1982; Wüthrich et al., 1984). As a general rule, the amide protons in peripheral β-strands are hydrogen bonded only on one side and display an alternating slow and fast exchange pattern, whereas the inner strands are hydrogen bonded to both sides and display slow exchange over their entire length (Wüthrich, 1986). The interstrand hydrogen bonding in the Tendamistat β-sheets (Kline & Wüthrich, 1985) is clearly seen in the exchange pattern of Figure 3.

A more detailed interpretation of the amide proton exchange data may be obtained from additional information relating to the mechanisms by which the exchange proceeds (Englander & Kallenbach, 1984; Hvidt & Nielsen, 1966; Wagner, 1983; Wagner & Wüthrich, 1979; Woodward et al., 1982). For each individual labile proton, we can write

$$\mathrm{N(H)} \underset{k_2}{\overset{k_1}{\rightleftharpoons}} \mathrm{O(H)} \xrightarrow{k_3} \mathrm{O(^2H)} \underset{k_1}{\overset{k_2}{\rightleftharpoons}} \mathrm{N(^2H)} \qquad (1)$$

N and O refer to the native and "open" states of the protein, respectively, where the proton in question would be freely accessible to the solvent in the states O. The rate constants k_1 and k_2 control the opening and closing of the protein, while k_3 relates to the chemical exchange from proton to deuterium. Two limiting situations are an EX1 mechanism, where $k_3 \gg k_2$, and an EX2 mechanism, where $k_2 \gg k_3$. k_3 is known to depend strongly on pH and temperature (Wüthrich, 1986), whereas k_1 and k_2 may be quite insensitive to the experimental conditions over a wide range. Therefore, different limiting situations can prevail in different regimes of pH and temperature. A recent detailed investigation with basic pancreatic trypsin inhibitor indicated that quite generally the observed slow exchange rates of polypeptide backbone amide protons, k_m, are related to an EX2 mechanism under conditions where the native form of globular proteins is preserved (Roder et al., 1985a). The observations described next show that the slow exchange rates in Tendamistat (Table I and Figure 3) are also due to EX2 processes.

A criterion for distinguishing between EX1 and EX2 exchange reactions relies on measurements on NOE's with labile protons in the partially deuteriated protein (Wagner, 1980; Roder et al., 1985). In the EX1 limit, neighboring amide protons in the three-dimensional structure show concerted exchange when exposed by an opening fluctuation, since $k_3 \gg k_2$. For any two amide groups which might be related by an ^1H–^1H NOE, one thus has either that both sites are protonated or that both sites are deuteriated. Only the former situation is capable of contributing to the intensity of the amide proton–amide proton NOESY cross-peak, and hence, the overall decrease of that cross-peak will be the same as for the NOESY cross-peaks between amide protons and nonexchanging protons. In contrast, in the EX2 limit, the exchange from neighboring amide sites is random and uncorrelated, resulting in a statistical distribution of ^1H and ^2H in pairs of nearby amide proton sites related by ^1H–^1H NOE's. After partial exchange, all the combinations ^1H–^1H, ^1H–^2H, ^2H–^1H, and ^2H–^2H will therefore be present. Since the two mixed states as well as the fully deuteriated state do not contribute to the NOE intensity, the NH–NH NOESY cross-peak intensity will decrease faster than that of the cross-peaks between a labile and a nonlabile proton. Such behavior is typical for the hydrogen-bonded β-sheet protons in Tendamistat. Figure 4 shows cross sections through the Tyr-46 NH position from two NOESY spectra recorded after exchange times of 0 and 2200 min. The exchange time for experiment B was chosen so that the exchange to deuterium would be approximately half complete for the most slowly exchanging β-sheet amide protons. The scaling of spectrum B has been adjusted so that the cross-peak with Cys-45 $C^\alpha H$ has the same height as in trace A. The two traces show the same relative peak heights for all NOE's of Tyr-46 NH with nonlabile protons. In contrast, the relative intensity of the cross-peak with Val-33 NH has significantly decreased and is barely above the noise in trace B. This and similar observations with different protons in Tendamistat indicate EX2 exchange and could not be ra-

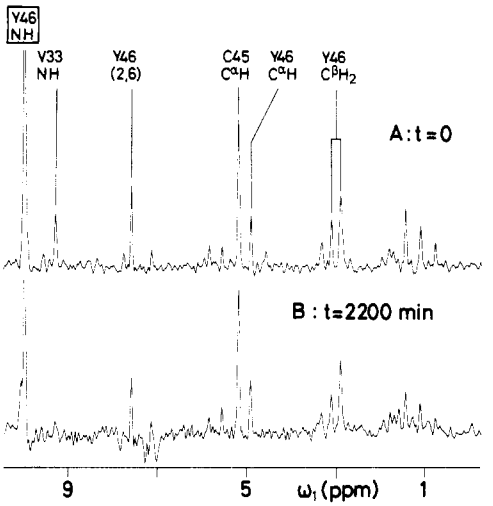

FIGURE 4: Cross sections along ω_1 at the chemical shift of Tyr-46 NH from two NOESY spectra recorded after different exchange times. The exchange times at 50 °C for each spectrum and the peak assignments are indicated in the figure. The plots have been scaled so that the cross-peak with Cys-45 $C^{\alpha}H$ has the same intensity in spectra A and B.

tionalized with the assumption of an EX1 mechanism.

In the EX2 limit, the observed exchange rate is given as (Hvidt & Nielsen, 1966)

$$k_m = \frac{k_1}{k_2} k_3 \qquad (2)$$

i.e., it corresponds to the product of the intrinsic exchange rate of the solvent-exposed amide group, k_3, and the equilibrium between open and closed states of the protein, k_1/k_2. By use of the standard values for k_3 (Molday et al., 1972), which were recently shown to be compatible with corresponding values measured directly in a denatured protein (Roder et al., 1985b), the equilibrium between states O and N in eq 1 can thus be evaluated from the data in Table I. This then enables one to investigate whether different labile protons are exposed to the solvent by structure fluctuations with identical values of k_1/k_2 or whether these are different for the individual protons. In plots of log k_m vs. log k_3, amide protons with identical equilibrium constants would all fall on the same straight line with slope 1, whereas different values for k_1/k_2 would be represented by different, parallel lines in such plots (Wagner, 1983; Wagner et al., 1984).

For Tendamistat, which contains two triple-stranded, antiparallel β-sheets (Kline & Wüthrich, 1985; Kline et al., 1986; Pflugrath et al., 1986), separate plots of k_m vs. k_3 (Figure 5) have been prepared for the two β-structures (Figure 6). For both sheets, there is considerable scattering of the k_1/k_2 values for the individual amide protons about straight lines with slope 1. Nonetheless, in view of the extent of scattering of the data points in previous, similar studies with different proteins (Wagner et al., 1984), it appeared justified to divide the amide protons in each β-sheet into three classes with diffeent average k_1/k_2 values. The locations of these protons in the β-sheets are identified in Figure 6. Clearly, the class of protons with the smallest values for k_1/k_2 dominates the central regions of both sheets, primarily the central strand and the inside faces of the peripheral strands. Somewhat larger values of k_1/k_2 prevail wherever the regular β-structure is perturbed, notably on the inside of the β-bulges and the hairpin turns, and between the strands with residues 7 and 8, and residues 70–72. High values for k_1/k_2 occur, quite naturally, for the exposed amide protons along the periphery of the two sheets, and for individual amide sites near the bulges and turns.

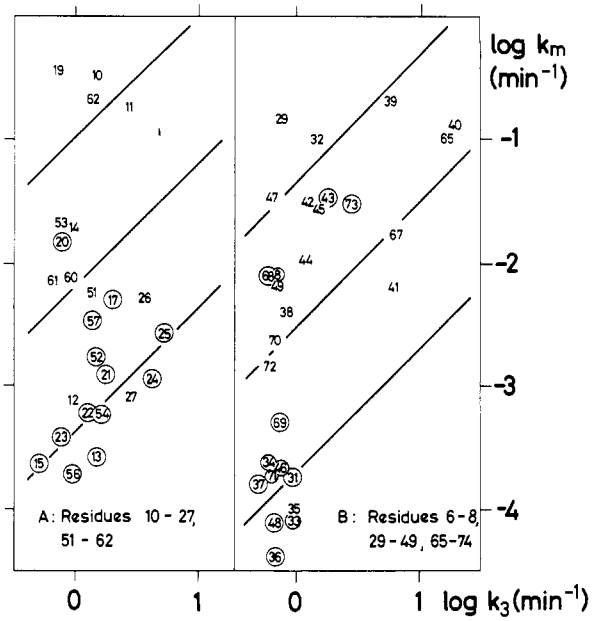

FIGURE 5: Logarithmic plots of the observed exchange rates, k_m, vs. the intrinsic exchange rates, k_3, for the two parts of the Tendamistat polypeptide chain outlined in Figure 6, each of which includes one of the two antiparallel β-sheets in this protein. The data points are identified by the sequence numbers. Those amide protons which form interstrand hydrogen bonds in the β-sheets (Figure 6) are circled. Three lines of slope 1 represent an average value for k_1/k_2 for three groups of amide protons in each β-sheet (see text and Figure 6).

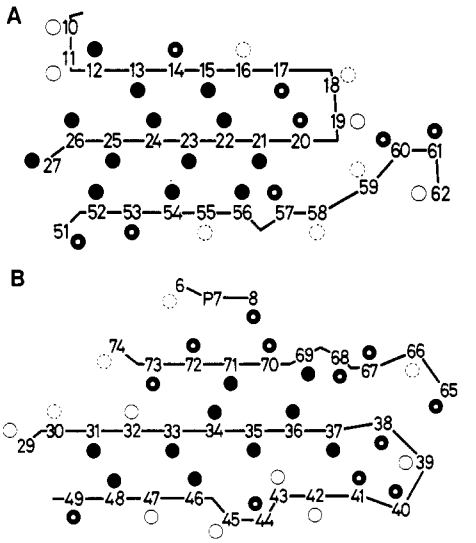

FIGURE 6: Schematic presentation of the amide proton exchange in two parts (A and B) of the Tendamistat polypeptide chain which include the two β-sheets. The polypeptide backbone is drawn as a straight lines jutting for the turns, bulges, and loops. The amide proton positions are indicated by circles. The amide protons were divided into four groups depending on their values for k_1/k_2. Closed circles identify those grouped around the lower lines in Figure 5. Open circles drawn with thick lines identify those grouped around the middle lines. Open circles with thin lines represent those grouped around the higher lines in Figure 5. Circles with broken lines identify amide protons seen only in H_2O solution.

Following previous work (Wagner, 1983; Wagner et al., 1984), the data of Figures 5 and 6 indicate that the exchange from the central regions of the β-sheets is dominated by a common, large-scale structure fluctuation, with some scatter of the data points around the lowest straight lines in Figure 5 arising from minor influences of superimposed local structure variations. Toward the ends of the β-sheets and near irregular structure features, such local fluctuations tend to dominate the global time variations, resulting in overall larger values

of k_1/k_2 and bigger scatter among the individual amide sites. An intriguing implication from comparison of panels A and B of Figure 5 is that the global fluctuation modes manifested in the k_1/k_2 values for the most slowly exchanging groups of amide protons are different for the two β-sheets, with the hydrogen-bonded amide protons in the sheet represented in Figure 5A showing generally higher k_1/k_2 values. Though the difference in the average k_1/k_2 values is within the scatter for each individual β-sheet, the large number of amide protons involved supports that the difference is significant, indicating that the fundamental fluctuation mode exposing the central region of one β-sheet in Tendamistat to the solvent leaves the other β-sheet largely unaffected, which in turn gets exposed to the solvent by a different, less frequent large-scale structure fluctuation. This observation is rather unexpected, since the three-dimensional structure of Tendamistat consists of a single antiparallel β-sheet barrel domain (Kline et al., 1986; Pflugrath et al., 1986).

Two additional comments relate to the aggregation of Tendamistat under the conditions used for the exchange measurements and the strategy used for the resonance assignments under these conditions. Self-aggregation at high protein concentration increases the effective molecular weight and thus leads to broadening of the NMR signal and decrease of the signal-to-noise ratio. While normally the lowering of the protein concentration would be expected to yield a decreased signal-to-noise ratio, selection of a lower concentration of Tendamistat in this studies resulted in an improved signal-to-noise ratio, showing that aggregation was thus successfully reduced. Protein aggregation can also affect the amide proton exchange rates, though for basic pancreatic trypsin inhibitor, where such effects were studied in more detail, this influence was limited to a few surface sites (Wagner, 1983; G. Wagner and K. Wüthrich, unpublished results). The conclusions drawn from the present study with Tendamistat center primarily on the interstrand hydrogen-bonded amide protons, which are less accessible to the surface, so that any remaining aggregation should be of only minimal importance.

Complete resonance assignments were previously obtained for Tendamistat at 50 °C and pH 3.2 (Kline & Wüthrich, 1986). In principle, the entire assignment procedure could have been repeated at the lower temperature used for the exchange studies (Figure 1), which would have required retaking the entire array of 2D NMR spectra and up to several months of analysis. The presently used approach, relying on comparison with the data at 50 °C, was much more efficient. It is a special advantage of the NMR procedure that its application to homologous sytems is highly effective, once a complete NMR study of a parent protein is available (Chazin et al., 1985; Stassinopoulou et al., 1984; Wüthrich, 1986).

ACKNOWLEDGMENTS

We thank Hoechst AG, Frankfurt am Main, West Germany, for an ample supply of Tendamistat and E. H. Hunziker-Kwik and R. Marani for careful preparation of the illustrations and the typescript.

Registry No. HOE-467, 86596-25-0; α-amylase, 9000-90-2.

REFERENCES

Aschauer, H., Vértesy, L., & Braunitzer, G. (1981) *Hoppe-Seyler's Z. Physiol. Chem. 362*, 465–467.

Chazin, W. J., Goldenberg, D. P., Creighton, T. E., & Wüthrich, K. (1985) *Eur. J. Biochem. 152*, 429–437.

Englander, S. W., & Kallenbach, N. R. (1984) *Q. Rev. Biophys. 16*, 521–655.

Hvidt, A., & Nielsen, S. O. (1966) *Adv. Protein Chem. 21*, 287–386.

Kline, A. D., & Wüthrich, K. (1985) *J. Mol. Biol. 183*, 503–507.

Kline, A. D., & Wüthrich, K. (1986) *J. Mol. Biol. 192*, 869–890.

Kline, A. D., Braun, W., & Wüthrich, K. (1986) *J. Mol. Biol. 189*, 377–382.

Molday, R. S., Englander, S. W., & Kallen, R. G. (1972) *Biochemistry 11*, 150–158.

Murai, H., Hara, S., Ikenaka, T., Goto, A., Arai, M., & Murao, S. (1985) *J. Biochem. (Tokyo) 97*, 1129–1133.

Neuhaus, D., Wagner, G., Vašák, M., Kägi, J. H. R., & Wüthrich, K. (1985) *Eur. J. Biochem. 151*, 257–273.

Pflugrath, J. W., Wiegand, G., Huber, R., & Vértesy, L. (1986) *J. Mol. Biol. 189*, 383–386.

Roder, H., Wagner, G., & Wüthrich, K. (1985a) *Biochemistry 24*, 7396–7407.

Roder, H., Wagner, G., & Wüthrich, K. (1985b) *Biochemistry 24*, 7407–7411.

Stassinopoulou, C. I., Wagner, G., & Wüthrich, K. (1984) *Eur. J. Biochem. 145*, 423–430.

Vértesy, L., & Tripier, D. (1985) *FEBS Lett. 185*, 187–190.

Vértesy, L., Oeding, V., Bender, R., Zepf, K., & Nesemann, G. (1984) *Eur. J. Biochem. 141*, 505–512.

Wagner, G. (1980) *Biochem. Biophys. Res. Commun. 97*, 614–620.

Wagner, G. (1983) *Q. Rev. Biophys. 16*, 1–87.

Wagner, G., & Wüthrich, K. (1979) *J. Mol. Biol. 134*, 75–94.

Wagner, G., & Wüthrich, K. (1982) *J. Mol. Biol. 160*, 343–361.

Wagner, G., Stassinopoulou, C. I., & Wüthrich, K. (1984) *Eur. J. Biochem. 145*, 431–436.

Wider, G., Hosur, R. V., & Wüthrich, K. (1983) *J. Magn. Reson. 52*, 130–135.

Woodward, C. K., Simon, I., & Tüchsen, E. (1982) *Mol. Cell. Biochem. 48*, 135–160.

Wüthrich, K. (1986) *NMR of Proteins and Nucleic Acids*, Wiley, New York.

Wüthrich, K., Štrop, P., Ebina, S., & Williamson, M. P. (1984) *Biochem. Biophys. Res. Commun. 122*, 1174–1178.